Exciton Stark and Landau ladders in a GaAs/Al$_x$Ga$_{1-x}$As superlattice

Z. Barticevic
Departamento de Física, Universidad Técnica Federico Santa María, Casilla 110-V, Valparaíso, Chile

M. Pachecho
Departamento de Física, Universidad de Santiago, Casilla 307, Santiago, Chile

F. Claro
Facultad de Física, Universidad Católica de Chile, Casilla 306, Santiago, Chile

We have calculated the excitonic optical absorption of a superlattice in the presence of electric and magnetic fields aligned with the superlattice axis. The main excitonic effects are an infrared shift and Stark/Landau ladder anticrossings. We show that an independent intrawell or interwell bidimensional exciton picture is accurate except when two transitions approach each other as the external fields are varied, in which case the interaction between these excitons causes the anticrossings previously observed in experiment.

I. INTRODUCTION

It was suggested a few years ago that the combination of Wannier-Stark and Landau quantization might produce interesting electronic conmensurability properties in a superlattice (SL).[1] An electric field aligned with the SL growth axis introduces a periodic sequence of resonances in the energy spectrum,[2,3] while a magnetic field pointing in the same direction quantizes the motion in the perpendicular plane, imposing a harmonic-oscillator-like structure in the spectrum. Two periods are thus present, one associated with the Wannier-Stark frequency and one with the cyclotron frequency. When the ratio between these frequencies is a rational the spectrum is periodic, while in the irrational case the additive structure of Wannier-Stark resonances and Landau levels is nonperiodic and dense.

The accurate manifestation of these properties in an actual sample in experiment depends on whether the assumptions of the model are realized. One knows that nonparabolicities of the dispersion law of electrons and holes, and the multiplicity of the relevant valence bands, produce distortions in the regularity of Landau levels already at moderate magnetic fields.[4] The spectrum is thus no longer characterized by periodic components, except at low magnetic fields.[5] Optical experiments also show that the various Wannier and Landau fans that develop in the energy spectrum as the fields are varied anticross rather than cross, suggesting that the spectrum is not the simple sum of two periodic structures as would be required to observe the commensurability properties.[6] This would be the case if the longitudinal and transverse degrees of freedom are not independent but coupled. In this paper, we study the effect of the largest coupling of this kind that occurs in an optical experiment in superlattices, that of the excited electron and the hole left behind. We show that away from possible crossings, this coupling modifies the energies by an approximately constant infrared shift that accounts for the exciton binding energy, while in the neighborhood of crossings the coupling is more severe and turns crossings into anticrossings as observed in experiment.

The properties of excitons in quantum-confined semiconductor structures have been studied in the past by several authors. In quantum wells the binding energy is large, since both electron and hole are localized within the well width.[7,8] In coupled asymmetric double quantum well systems the electron and hole may be in the same or in different wells, giving rise to two distinct binding energy states. If an electric field is applied along the growth axis, the Stark shift produces a crossing in the energy of these states.[9] The case of semiconductor superlattices has also been discussed in the past in the presence of an electric field.[10-12] The binding energy of the exciton depends on the barrier width, height, and applied electric field, since these quantities control the degree of localization of the wave functions. We here develop a formalism that includes a magnetic field aligned with the SL axis. Neglecting the coupling between hole bands, we find that the Wannier-Stark localization allows a description in terms of pseudo-bi-dimensional excitons, each with the electron and the hole placed in well defined SL layers that need not be the same. This gives rise to the distinction between *interwell* and *intrawell* excitons. We also show that anticrossings are due to the coupling between these special excitons.

In Sec. II, we present a method for calculating the excitonic envelope wave function for a SL in the presence of an electric and a magnetic field parallel to the growth axis. We work in the effective mass approximation and assume a parabolic dispersion for electrons and a four band model for holes. We apply our method to calculate the excitonic spectrum and the envelope wave functions for heavy-hole and light-hole excitons, for different values of the external fields. In Sec. III, we discuss the excitonic

<u>51</u>   14 414

optical absorption spectrum in terms of the above formalism and present numerical results for the binding energies and the optical absorption of excitonic states. Comparison of our results with available experimental data shows excellent agreement.

II. EXCITONIC ENVELOPE FUNCTION

In this section, we sketch the method[13] we follow to obtain the excitonic eigenstates of a SL in the presence of a magnetic (B) and an electric (F) field both parallel to the growth axis. The SL period is d and we take the z axis to be along the direction of growth. In the effective mass approximation the excitonic wave function may be written as a linear combination of products of electron- and hole-Bloch functions. The excitonic Hamiltonian reduces then to the sum of single particle electron and hole Hamiltonians, and the screened Coulomb interaction. For a GaAs/Al$_x$Ga$_{1-x}$As SL the bands relevant to optical transitions have Γ_6 and Γ_8 edge symmetry. For these materials it is a good approximation to neglect the split off Γ_7 band and the coupling between conduction and valence bands. In this case, the excitonic envelope function components $F_{MM'}$ are solutions of the matrix differential equation,

$$\sum_{L,L'} (H^{\mathrm{exc}})_{MM',LL'} F_{LL'} = E_{\mathrm{exc}} F_{MM'}. \quad (1)$$

Here, H^{exc} is the effective mass Hamiltonian operator.[14] It includes the kinetic energy of the conduction-band electron and the valence-band hole in the presence of the magnetic field, the screened electron-hole (e-h) Coulomb interaction, the external electric field, and the SL potential. The summation over L includes the spin up or down terms corresponding to the Γ_6 conduction band, and the sum over L', the four spin states of the Γ_8 spin-orbit split valence band. If we neglect the small contribution of the e-h exchange interaction, the eight-dimensional matrix equation (1) reduces to two four-dimensional equations for both spin states of the conduction band. The excitonic envelope function components $F_{MM'}$ depend on the e-h relative coordinates $\vec{\rho} = (\rho, \phi)$ for motion parallel to the SL layers, as well as on the coordinates for motion along the z axis. We expand these components in terms of single-particle solutions of the effective mass equation for motion along the SL axis in the presence of the electric field alone. In the tight-binding approximation, taking into account one level per well only, these functions have the form[1]

$$\Phi^{m,M}(z) = \sum_l J_{l-m}(\eta)\, \phi_M(z-ld). \quad (2)$$

Here, $\phi(z-ld)$ is the lowest energy eigenstate of the quantum well associated with a period of the SL centered at $z = ld$, and $J_n(\eta)$ is the Bessel function of order n, with η the ratio between the transfer energy between neighboring wells and the Stark energy $\Delta = eFd$. The single-particle energy associated with this eigenstate is of the form $\epsilon_F = \epsilon_0 + m\Delta$, the integer m denoting the Stark

quantum number. Due to the electric field induced localization, Eq. (2) describes an electron or a hole primarily confined about $z = md$. In terms of these functions, our expansion reads

$$F_{MM'}(\vec{\rho}, z_e, z_h) = \sum_{mm'} C_{MM'}^{mm'}(\rho, \phi)\Phi_e^{m,M}(z_e)\, \Phi_h^{m',M'}(z_h),$$

$$(3)$$

where the subindices e, h, refer to electrons and holes, respectively. Note that the coefficients in this expansion depend on the in-plane *relative* electron- ($\Phi_e^{m,M}(z_e)$), and hole- ($\Phi_h^{m',M'}(z_h)$) coordinates only.

It is easy to show that the excitonic Hamiltonian is invariant under a simultaneous shift of z_e and z_h by nd, with n an integer. The excitonic envelope functions satisfy then the special form of Bloch's theorem,

$$F_{MM'}^q(\vec{\rho}, z_e + nd, z_h + nd) = e^{iqnd}\, F_{MM'}^q(\vec{\rho}, z_e, z_h). \quad (4)$$

Here, q is the exciton wave number in the z direction. Using this theorem and the general property $\Phi^{m,M}(z) = \Phi^{0,M}(z-md)$, one can show that the function $F_{MM'}^q$ may be written in the form

$$F_{MM'}^q = \sum_\ell C_{MM'}^{0\ell}(\rho, \phi)\, f_{MM'}^{\ell q}(z_e, z_h), \quad (5)$$

where

$$f_{MM'}^{\ell q}(z_e, z_h) = \frac{1}{\sqrt{N}} \sum_m e^{iqmd}\, \Phi_e^{m,M}(z_e)\Phi_h^{\ell+m,M'}(z_h).$$

The index ℓ denotes the difference between the Stark quantum numbers of the electron and the hole. Due to the localization of the functions $\Phi^{m,M}(z)$, this index essentially corresponds, in units of the SL period, to the spatial separation between them. The function $f_{MM'}^{\ell q}(z_e, z_h)$ can be seen as a linear combination of noninteracting e-h pairs a distance ℓ apart from each other.

For simplicity, we shall next apply our method to independent excitons, that is, we discard the off-diagonal elements in the hole Hamiltonian. In this case, Eq. (1) becomes a scalar equation. In particular, for heavy-hole excitons the effective mass Hamiltonian operator is given by

$$H^{\mathrm{exc}} = -\frac{1}{m_e}\frac{d^2}{dz_e^2} + V_e(z_e) - \frac{1}{m_{\mathrm{hh}}}\frac{d^2}{dz_h^2} + V_h(z_h)$$

$$+(z_e - z_h)eF + \frac{1}{m_1}\left(-\nabla_\rho^2 + \frac{\gamma^2\rho^2}{4}\right) + \frac{1}{m_2}\gamma L_z$$

$$+3\kappa\gamma - \frac{2}{\epsilon|\vec{r_e} - \vec{r_h}|} + \frac{g_e\gamma}{2}, \quad (6)$$

where the electron (m_e) and heavy-hole (m_{hh}) effective masses are in units of the bare electron mass, lengths are in Bohr units, and energies are in units of Rydbergs. Also, $m_1 = (1/m_e + \gamma_1 + \gamma_2)^{-1}$ and $m_2 = (1/m_e - \gamma_1 - \gamma_2)^{-1}$, with γ_1, γ_2, and κ the valence band Luttinger parameters, and g_e the g factor of the conduction-band electron. ϵ is an average static dielectric constant of the two materials, V_e and V_h are the electron and hole SL

potentials, and γ the dimensionless energy of the free electron lowest Landau level.

Using expansions (5) and (6) in Eq. (1), we obtain for the coefficients

$$\left[\frac{1}{m_1}\left(\nabla_\rho^2 + \frac{\gamma^2\rho^2}{4}\right) + \frac{1}{m_2}\gamma L_z\right] C_{e,hh}^{0\ell}(\rho,\phi)$$

$$+ \sum_{\ell'} M_{\ell\ell'}(\rho)\, C_{e,hh}^{0\ell'}(\rho,\phi) = (E - \ell eFd)\, C_{e,hh}^{0\ell}(\rho,\phi). \tag{7}$$

Here, $E = E_{exc} - E_0^e - E_0^v - E_g - \gamma(3\kappa \pm \frac{g_e}{2})$, where $E_0^e(E_0^v)$ is the first energy level of the electron (hole) in the quantum well, and E_g is the energy gap. The matrix elements of the e-h interaction energy are

$$M_{\ell,\ell'}(\rho) = \left\langle f_{e,hh}^{\ell q} \left| \frac{2}{\epsilon\sqrt{\rho^2 + (z_e - z_h)^2}} \right| f_{e,hh}^{\ell' q} \right\rangle \tag{8}$$

and are given in Appendix A.

If in Eq. (7) the diagonal terms $\ell = \ell'$ are considered only, the index ℓ becomes a good quantum number, and the problem is reduced to one of independent pseudo-bidimensional excitons in a magnetic field. We call such excitons "Stark excitons," since they arise naturally in our basis set of localized Wannier-Stark eigenfunctions for motion along the SL axis. In fact, in this diagonal approximation, the Coulomb interaction in Eq. (7) has been averaged out over the z axis and what remains may be thought of as an electron and a hole, each constrained to move over layers a distance ℓd apart from each other. Equation (7) describes the dynamics in the x-y plane of the interacting pair in a magnetic field, and is thus of pure two-dimensional character. For each value of ℓ there is a set of solutions with eigenvalues $\epsilon_{i\ell} = E_i^\ell - \ell eFd$, and, therefore, the complete spectrum is the sequence of ladders $E_i^\ell = \epsilon_{i\ell} + \ell eFd$. In the large magnetic field limit, the index i may be associated with the usual Landau index of noninteracting particles in a magnetic field. At certain values of the external fields, the ladders will cross. It is in the neighborhood of these crossings where the off-diagonal Coulomb terms $M_{\ell\ell'}$ become important and, in fact, cause a repulsion of levels and therefore, anticrossings. We have found that away from these crossings such elements do not change significantly the eigenenergies and could be ignored completely. The off-diagonal matrix elements in Eq. (7) couple an ℓ-Stark exciton and an ℓ'-Stark exciton, and it is this coupling that turns crossings of levels into the anticrossings observed in experiment.[6]

In order to solve Eq. (7), we expand the coefficients $C_{e,hh}^{0\ell'}(\rho,\phi)$ in a restricted set of Gaussian functions with length parameters λ_j, fixed a priori to cover the physical range of relevant radii and assure convergence,

$$C_{e,hh}^{0\ell s}(\rho,\phi) = \sum_j a_j^\ell \frac{e^{is\phi}}{\sqrt{2\pi}} \left(\frac{\rho}{i}\right)^{|s|} e^{-\frac{\rho^2}{\lambda_j^2}}, \tag{9}$$

where s is an integer associated with the conserved z component of the total angular momentum. Replacing (9) in (7), we obtain

$$\sum_j a_j^{\ell'} \frac{|s|!}{\beta^{|s|+2}} \left[\frac{\gamma s\beta}{2m_2} + \frac{(|s|+1)\gamma^2}{8m_1}\right.$$

$$\left. + \frac{2(|s|+1)}{m_1\lambda_j^2\lambda_k^2} - \frac{(E + \ell eFd)}{2}\beta\right]$$

$$+ \frac{2}{\epsilon\pi}\sum_\ell \sum_j a_j^\ell \frac{|s|!}{\beta^{|s|+1}} S_s^{\ell\ell'}(\beta) = 0. \tag{10}$$

Here, $\beta = 1/\lambda_j^2 - 1/\lambda_k^2$ and

$$S_s^{\ell\ell'}(\beta) = \int_0^\infty \int_0^\infty \xi \exp(-\xi^2/4\beta) L_{|s|}^0 \left(\frac{\xi^2}{4\beta}\right)$$

$$\times \frac{N(\ell,\ell',\alpha)}{\alpha^2 + \xi^2}\, d\alpha d\xi, \tag{11}$$

where $L_{|s|}^0(\frac{\xi^2}{4\beta})$ is the Laguerre polynomial and

$$N(\ell,\ell',\alpha) = \int_0^\infty \int_0^\infty \cos[\alpha(z_e - z_h)] f_{e,hh}^{*\ell'q}(z_e, z_h)$$

$$\times f_{e,hh}^{\ell q}(z_e, z_h) dz_e dz_h. \tag{12}$$

To solve Eq. (10), we need to restrict the basis by choosing an upper value of $|\ell| = \ell_{max}$. It is clear, due to the Stark localization, that the coupling between an ℓ exciton and an ℓ' exciton will be dominated by nearest neighbor excitons. On the other hand, the absorption oscillator strength will be very small for large ℓ, because of the small overlap between the electron and hole wave functions. For the fields considered below, we have checked in our numerical calculations that truncation at $|\ell_{max}| = 3$ gives sufficient accuracy. In fact, increasing this number by two changes the excitation energies by less than 0.01%.

III. ABSORPTION COEFFICIENT

We may now apply the above formalism to obtain the excitonic optical absorption coefficient. It is given by[15]

$$\alpha(\omega) = \sum_n \frac{4\pi e^2|\xi\dot{P}_{cv}|^2}{\omega m_0^2\eta(\omega)c} O_n^{exc} \delta(E_n - \hbar\omega), \tag{13}$$

where ξ is the photon polarization, P_{cv} the electron momentum operator, $\eta(\omega)$ the refractive index and m_0 the bare electron mass. The oscillator strength O_n^{exc} is given by

$$O_n^{exc} = \sum_q \frac{1}{Nd} \left|\int_{-\infty}^\infty dz F_{e,hh}^q(o, z, z)\right|^2. \tag{14}$$

Using Eq. (5) and the properties of Bessel functions, we obtain

$$O_n^{exc} = \delta_{q,0}\, \delta_{s,0} \sum_{\ell\ell'} \sum_{ii'} a_i^\ell a_{i'}^{\ell'} \sum_{pp'} J_{p-\ell}(\eta^h$$

$$-\eta^e) J_{p'-\ell'}(\eta^h - \eta^e)\, \mu(p')\, \mu(p), \tag{15}$$

where a_i^ℓ are the solutions of Eq. (10), $\eta^{e(h)}$ is the

transfer energy between neighboring wells, and $\mu(p) = \int dz\, \phi_e(z)\phi_h(z-pd)$ are the overlap integrals for the well eigenstates.

In what follows, we present numerical results for heavy- and light-hole excitons in a $GaAs/Al_xGa_{1-x}As$ SL, for which there is experimental data available. In our calculations the band gap of GaAs is taken to be $E_g = 1.52$ eV and we assume a valence-band offset of 30%, and a band-gap discontinuity as given by the expression $\Delta E_g = 1.36x + 0.22x^2$. The effective mass parameters for GaAs(AlAs) are $m_e = 0.067(0.15)$, $m_{lh\perp} = 0.11(0.13)$, $m_{hh\perp} = 0.34(0.42)$, and $\epsilon = 12.0(9.8)$. In addition, we set the in-plane effective mass for the heavy exciton $m_{hh}^{exc} = 0.06$ and for the light-hole exciton $m_{lh}^{exc} = 0.069$.

As a first test of our model, we have calculated the absorption spectrum in the zero magnetic field limit. For this case, we have compared our results with photocurrent data reported by Agulló-Rueda et al. for a 40 Å GaAs/20 Å $Al_{0.35}Ga_{0.65}As$ SL.[16] We find excellent agreement between theory and experiment if we use the geometrical parameters suggested by Dignam and Sipe for the same sample, that is, a layer thickness of 41 Å for the well, and 24 Å for the barrier.[17] In Figs. 1(a) and

1(b), we show the experimental (circles) and calculated (dots) excitonic transition energies as a function of the electric field for heavy- and light-hole excitons. In this case, as Dignam and Sipe have done, we have also adjusted the zero of the electric field in 1.5 kV/cm.

Photocurrent experimental data of excitonic transitions in a 40 Å GaAs/20 Å $Al_{0.35}Ga_{0.65}As$ SL under longitudinal electric and magnetic fields have been reported by Alexandrou, Mendez, and Hong.[6] The following results are for this system. Figure 2 shows results for the excitonic absorption strength as a function of the photon energy for different values of the magnetic field and an electric field of 33.8 kV/cm. To account for thermal and other broadening effects, we have replaced in our calculations the δ functions in Eq. (13) by Lorentzian curves of width 2.5 meV. The optical spectrum shows excitonic resonances associated with bound states of an electron and a hole localized in the same well, or in neighboring wells of the SL. For zero magnetic field, we see the main Stark transitions clearly resolved. They are labeled with the symbol ℓhh, where the integer ℓ is as defined before. When the magnetic field is increased, new excitations of the system associated with each Stark transition appear. For finite magnetic field, we have labeled the peaks with the symbol $(n, \ell hh)$, where, for a given ℓhh, the integer n orders the transitions according to increasing energy. Thus, for example, $(0, 0hh)$ is associated with the lowest intrawell excitonic transition and $(1, -1hh)$ labels
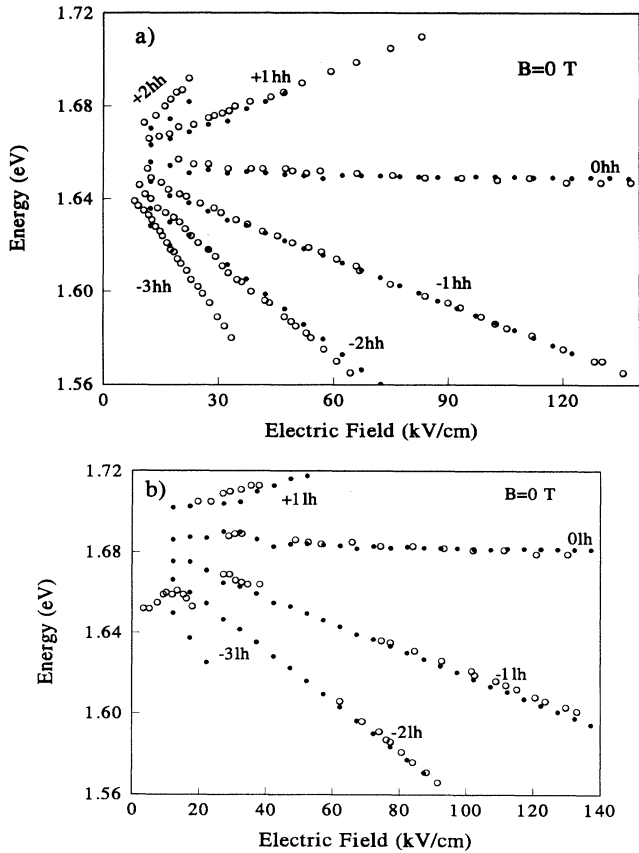

FIG. 1. Calculated (a) heavy-hole and (b) light-hole excitonic transitions energies for a 41 Å GaAs/24 Å $Al_{0.35}Ga_{0.65}As$ SL at zero magnetic field, as a function of the applied electric field. Open circles are the experimental photocurrent data from Ref. 16. All figures refer to the same SL.
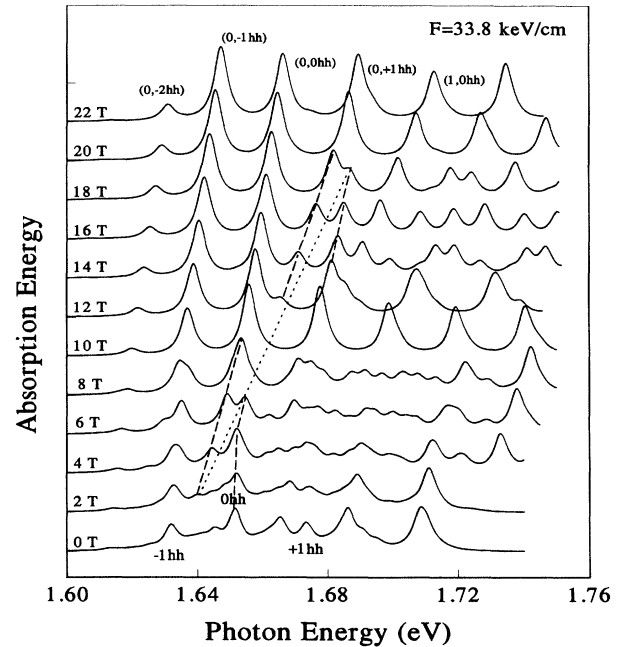

FIG. 2. Absorption coefficient for different values of the magnetic field at a constant electric field. The dotted line shows the $(1, -1hh)$ transition as it would appear without electron-hole interaction. The dashed lines show anticrossings as a function of the magnetic field. The $(1, -1hh)$ transition anticrosses with the $(0, 0hh)$ transition around 6 T, and with the $(0, +1hh)$ transition around 16 T. Both fields are parallel to the SL growth axis.

the second *interwell* excitonic transition. Below 4 T the $(0, 0hh)$ transition is strong, while the $(1, -1hh)$ is weak. As the magnetic field is increased, the peaks associated with these two transitions approach each other, their intensities become comparable, and above 6 T their relative strength is inverted.

The magnetic field regions for which the excitation energy of an *intrawell* exciton and an *interwell* exciton are similar are observed as zones of anticrossings in Fig. 3, where we have plotted the transition energies as a function of magnetic field. These regions of anticrossings occur, in general, whenever the energy of the magnetic excitonic transition is close to a multiple M of the Stark energy. For the corresponding magnetic field, anticrossings will be observed between the transitions $(n, \ell hh)$ and $(n \pm M, \ell hh \mp M)$, with $(n \pm M) > 0$. In the one-particle model, where excitonic effects are neglected, those transitions cross as a function of magnetic field,[5] the e-h interaction being the relevant coupling that turns crossing into anticrossings.

We also include in Fig. 3 the photocurrent peak data of Alexandrou, Mendez, and Hong,[6] reported for a 40 Å GaAs/20 Å $Al_{0.35}Ga_{0.65}Al$ SL in an electric field of 30 kV/cm. As in the case of zero magnetic field, we found the best agreement with the experiment by using the geometrical parameters suggested by Dignam *et al.*, and by setting the field at a value of 33.8 kV/cm, which means to adjust the zero of the field in 3.8 kV/cm. For magnetic fields B less than 12 T, the calculated excitonic peak positions as a function of the field are in excellent agreement with the experimental data. For higher magnetic fields the agreement is less satisfactory, because the coupling of heavy- and light-hole states has not been included in our calculations. This coupling leads to quantum well hole energies, whose magnetic field dependence departs significantly from the linear free electron result above about 7 T, as we have shown in Ref. 5. This

effect leads to a magnetic field dependent excitonic effective mass, such that in the limit of high magnetic field it approaches the electron effective mass.

In Fig. 4, we have plotted the transition energies as a function of the applied electric field for the same SL in a magnetic field of 21.4 T. In this figure, we have included both the calculated (solid circles) and experimental (open circles) data, for light- and heavy-hole excitons. In this case, we have used the excitonic effective masses $m_{hh}^{exc} = 0.067$ and $m_{lh}^{exc} = 0.0689$, to take into account the effect of coupling of heavy and light hole disscused above.

Binding energies of the exciton may also be obtained in our formalism. For zero magnetic field, our results are in good agreement with the results of Dignam and Sipe for an electric field of 33.8 keV/cm.[17] We have observed the asymmetry in the binding energies of the exciton states $(0, +Mhh)$ and $(0, -Mhh)$ predicted by them. Our results also show that the $(0, 0hh)$ exciton is the most bounded, with a binding energy of 7.9 meV, while the $(0, -1hh)$ exciton has a binding energy of 6.5 meV. For this last case, Alexandrou *et al.* have estimated an experimental value of 6.7 ± 1 meV,[6] which again confirms the agreement of theory and experiment.

When the magnetic field is increased, the in-plane excitonic radius of a Stark exciton decreases and its binding energy grows. For certain values of the magnetic field the coupling between an ℓ-type Stark exciton and an $(\ell - 1)$-type Stark exciton becomes relevant and the binding energy as a function of the field shows very clearly the conversion of the ℓ-type excitonic state to the $(\ell - 1)$-type excitonic state, and vice versa. In Fig. 5, we show the ground state binding energies of the $\ell = 0$ (full line) and $\ell = -1$ (dashed line) excitons if the coupling between the Stark excitons is neglected. The dots are for the fully coupled system and show a binding energy with some struc-
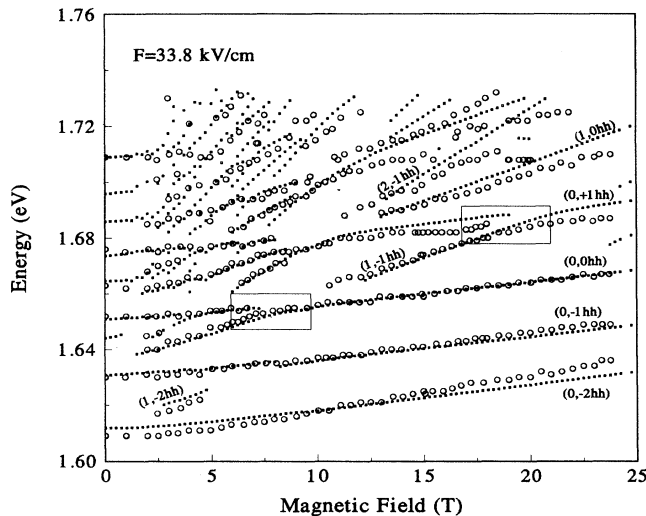

FIG. 3. Excitonic transition energies as a function of the magnetic field for an electric field of $F = 33.8$ kV/cm. Open circles are experimental data from Ref. 6 and solid circles are our results.
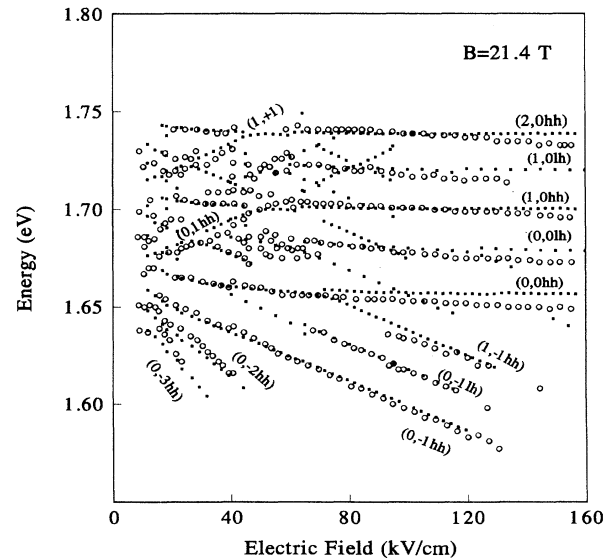

FIG. 4. Excitonic transition energies as a function of the electric field for a constant magnetic field $B = 21.4$ T. Open circles are experimental data from Ref. 6 and solid circles are our results.
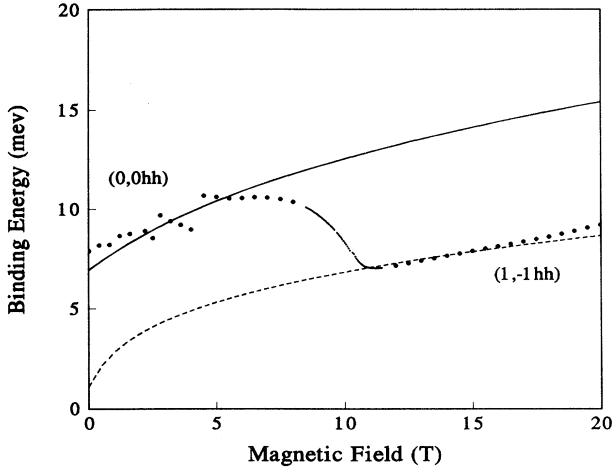
FIG. 5. Binding energies for the 0hh state as a function of the magnetic field in an electric field of $F = 33.8$ kV/cm. The solid and dashed lines correspond to the 0hh and -1hh states, respectively, neglecting the coupling between them.

ture revealing anticrossings. While below 7 T the dots roughly follow the uncoupled $\ell = 0$ exciton, they are seen to switch rather sharply to the $\ell = -1$ uncoupled exciton in the region between 7 T and 11 T corresponding to the main anticrossing highlighted in Fig. 3. At other values of the magnetic field, a similar behavior in the binding energy can be observed because of the coupling of the intrawell exciton $(0, 0hh)$ with other $\ell \neq 0$ interwell excitons. For example, for fields below 7 T the intrawell Stark exciton $(0, 0hh)$ also couples weakly with the interwell Stark excitons $(2, -1hh)$ and $(3, -1hh)$. This can be observed as little discontinuities in the binding energy in Fig. 5.

To summarize, we have developed a formalism appropriate for the calculation of the excitonic optical absorption of a superlattice in the presence of an electric and a magnetic field, both aligned with the superlattice axis. We have applied this formalism to a GaAs/Al$_x$Ga$_{1-x}$As sample for which experimental data is available and have found excellent agreement between our results and experiment.[6] The spectrum contains Stark (Landau) fans that develop when the electric (magnetic) field is increased, already predicted by the one-electron picture.[1] The excitonic formation causes an infrared shift in the spectrum and turns the crossings given by the one-electron approximation into anticrossings. A convenient picture to use involves bidimensional excitons with the electron and the hole moving in separate planes, and we find that it is the interaction between these excitons that turns crossings into anticrossings in the spectrum.

APPENDIX A

In this appendix, we outline the procedure used to evaluate the matrix elements of the Coulomb interaction. We have to calculate

$$M_{\ell,\ell'}(\rho) = \left\langle f_{e,hh}^{lq} \left| \frac{2}{\epsilon\sqrt{\rho^2 + (z_e - z_h)^2}} \right| f_{e,hh}^{l'q} \right\rangle. \quad (A1)$$

We express the Coulomb interaction in terms of the Fourier integral,

$$\frac{1}{\sqrt{\rho^2 + (z_e - z_h)^2}} = \frac{1}{\pi^2} \int_0^{2\pi} \int_0^\infty \int_0^\infty e^{i\xi\rho\cos\theta}$$
$$\times \xi \frac{\cos\alpha(z_e - z_h)}{\alpha^2 + \xi^2} d\xi d\theta d\alpha. \quad (A2)$$

By performing the integral over θ, we obtain

$$\frac{1}{\sqrt{\rho^2 + (z_e - z_h)^2}} = \frac{1}{\pi^2} \int_0^\infty \int_0^\infty J_0(\xi\rho)$$
$$\times \xi \frac{\cos\alpha(z_e - z_h)}{\alpha^2 + \xi^2} d\xi d\alpha. \quad (A3)$$

The matrix elements given by Eq. (A1) can be written in the form

$$M_{\ell,\ell'} = \frac{4}{\epsilon\pi} \int_0^\infty \int_0^\infty \int_0^\infty \xi J_0(\xi\rho) \frac{N(\ell,\ell',\alpha)}{\alpha^2 + \xi^2} d\alpha d\xi, \quad (A4)$$

where $J_0(\xi\rho)$ is the zero-order Bessel function and $N(\ell,\ell',\alpha)$ is given in Eq. (12). Because the function $f_{e,hh}^{*\ell q}$ involves only exponential (out of the well), and harmonic (in the well), functions, the integral $N(\ell,\ell',\alpha)$ can be performed analytically. We find

$$N(\ell,\ell',\alpha) = \sum_n [Q_1(l,l',n)D(A_\nu^c, A_{\nu'}^v, n)$$
$$+ Q_2(l,l',n)G(A_{\nu'}^v, C_\nu^c, n)$$
$$+ Q_1(l,l',n+1)G(A_\nu^c, C_{\nu'}^v, -n)], \quad (A5)$$

with

$$D(A_\nu^c, A_{\nu'}^v) = A_\nu^c A_{\nu'}^v g_2(k_\nu, \alpha) g_2(k_{\nu'}, \alpha) \quad (A6)$$

and

$$G(A_{\nu'}^v, C_\nu^c, n) = A_{\nu'}^v C_\nu^c \sum_{j=0,1} \sum_{m=1}^4 (-1)^{m+1} e^{-[d+(-1)^m \chi_\nu]} g_2(k_{\nu'}, \alpha)$$
$$\times g_1 \left(\chi_\nu, \alpha + (-1)^{\frac{(m-1)(m-2)}{2}} k_\nu, (-1)^m - \frac{(-1)^j(j-n)d\alpha}{\left(\alpha + (-1)^{\frac{(m-1)(m-2)}{2}} k_\nu\right)} \right) \quad (A7)$$

Here, $k_\nu(k_{\nu'})$ and $\chi_\nu(\chi_{\nu'})$ denote the electron (hole) wave vectors in the quantum well and the barrier, respectively. Also, $A^c_\nu(A^v_{\nu'})$ and $C^c_\nu(C^v_{\nu'})$ are normalization constants for electrons (holes) localized in neighboring wells. The functions $g_1(x,y,z)$ and $g_2(x,y)$ are defined as

$$g_1(x,y,z) = \left[\frac{x\cos(yz) - y\sin(yz)}{x^2 + y^2}\right], \qquad (A8)$$

$$g_2(x,y) = \frac{1}{2}\left[\frac{x\sin(x)\cos(y) - y\sin(y)\cos(x)}{x^2 - y^2} + \frac{\sin y}{y}\right], \qquad (A9)$$

and the functions $Q_1(l,l',n)$ and $Q_2(l,l',n)$ are combi-nations of Bessel functions given by

$$Q_1(l,l',n) = N J_{l'-n}(\eta^e - \eta^h) J_{l-n}(\eta^e - \eta^h), \qquad (A10)$$

$$Q_2(l,l',n) = Q_1(l,l'+1,n) + Q_1(l',l+1,n), \qquad (A11)$$

with

$$\eta^{e(h)} = v_{e(h)} \int_{-\frac{L}{2}}^{\frac{L}{2}} \phi(z)_{e(h)}\phi(z-d)_{e(h)}\, dz. \qquad (A12)$$

Here, $v_{e(h)}$ is the magnitude of the conduction-(valence-)band discontinuity. To obtain Eq. (A4), we have assumed $q = 0$, since these are the only states which are accessible via optical excitation.

[1] F. Claro, M. Pacheco, and Z. Barticevic, Phys. Rev. Lett. **64**, 3058 (1990).

[2] G. H. Wannier, Phys. Rev. **117**, 432 (1960).

[3] E. E. Mendez, F. Agulló-Rueda, and J. M. Hong, Phys. Rev. Lett. **60**, 2426 (1988).

[4] M. Altarelli, in *Heterostructures and Semiconductor Super-lattices*, edited by G. Allan, G. Bastard, N. Boccara, and M. Voos (Springer, Berlin, 1986).

[5] M. Pacheco, Z. Barticevic, and F. Claro, Phys. Rev. B **46**, 15 200 (1992).

[6] A. Alexandrou, E. E. Mendez, and J. M. Hong, Phys. Rev. B **44**, 1934 (1991).

[7] G. Bastard, E. E. Mendez, L. L. Chang, and L. Esaki, Phys. Rev. B **26**, 1974 (1982).

[8] G. D. Sanders and Y. C. Chang, Phys. Rev. B **32**, 5517 (1985).

[9] R. P. Leavitt and J. W. Little, Phys. Rev. B **42**, 11 774 (1990).

[10] N. F. Johnson, J. Phys. Condens. Matter **2**, 2099 (1990).

[11] R. P. Leavitt and J. W. Little, Phys. Rev. B **42**, 11 784 (1990).

[12] M. M. Dignam and J. E. Sipe, Phys. Rev. Lett. **64**, 1797 (1990).

[13] M. Pacheco, Z. Barticevic, and F. Claro, J. Phys. C **5**, A393 (1993).

[14] G. E. W. Bauer and T. Ando, Phys. Rev. B **38**, 6015 (1988).

[15] M. M. Dignam and J. E. Sipe, Phys. Rev. B **41**, 2865 (1990).

[16] F. Agulló-Rueda, E. E. Mendez, and J. M. Hong, Phys. Rev. B **40**, 1357 (1989).

[17] M. M. Dignam and J. E. Sipe, Phys. Rev. B **43**, 4097 (1991).